

A numerical model of a towed cable-body system

C. K. H. Chin* R. L. May* H. J. Connell*

(Received 7 August 2000)

Abstract

In this paper, the motion of a body towed by an aircraft on a long thin elastic cable is modelled. The motion of the cable is described by a system of partial differential equations, and a six degree of freedom model used for the towed body. The partial differential equations governing the motion of the cable-body system are solved numerically

* Department of Mathematics, RMIT University, GPO Box 2476V, Melbourne, Victoria 3001, AUSTRALIA. <mailto:chris.chin@rmit.edu.au>, <mailto:rob@ems.rmit.edu.au> and <mailto:howard.connell@rmit.edu.au>

⁰See <http://anziamj.austms.org.au/V42/CTAC99/Chin> for this article and ancillary services, © Austral. Mathematical Soc. 2000. Published 27 Nov 2000.

by discretising them using the finite difference method. The resulting system of non-linear equations is solved iteratively at each time step.

The numerical scheme, which allows for the deployment or retrieval of the cable, is briefly described and results presented for several manoeuvres of the towing aircraft.

Contents

1 Introduction	C364
2 Mathematical Model	C365
3 Numerical Scheme	C371
4 Results	C373
5 Conclusions	C383
References	C383

1 Introduction

Towed bodies are frequently deployed from aircraft on thin cables up to several kilometres in length. These bodies can be used as targets or may be part of the aircraft's defence system by acting as decoys for missiles. Accurate prediction of the position of the body and the tension in the cable as the aircraft manoeuvres is needed, not only for safety considerations, but also in order to design the various components of the towing system.

Several approaches have been used to model towed cables. The motion of the cable can be described by a system of partial differential equations [1], or the cable can be considered either as a number of inextensible rods connected by frictionless hinges [7] or as “lumped” masses connected by inextensible links having no mass [2]. The first approach was used in [4] to model a body being towed behind an aircraft by an elastic cable, but only a simple model of the towed body was used. This paper extends that work by incorporating a six degree of freedom model of the towed body.

As before the cable is assumed to be homogeneous and have a constant diameter in its unstretched state. The model allows deployment or retrieval of the cable while the towing aircraft follows a prescribed manoeuvre in three dimensions.

2 Mathematical Model

The aircraft is assumed to be at the origin of a fixed reference frame (x, y, z) at time $t = 0$, with the x axis pointing in the direction of the horizontal component of the initial velocity and z points vertically downwards. Unit vectors in the x, y and z directions are denoted by $(\mathbf{i}, \mathbf{j}, \mathbf{k})$ as shown in Figure 1. An orthonormal set of unit vectors $(\mathbf{t}, \mathbf{n}, \mathbf{b})$ is defined at each point on the cable with \mathbf{t} tangential to the cable and \mathbf{n} normal to the cable and lying in a vertical plane. The orientation of the local system a distance s along the unstretched cable from the towed body end at time t is described with the aid of the Euler angles $\theta(s, t)$ and $\phi(s, t)$. Rotating the local axes through an angle ϕ about \mathbf{b} then rotating them through θ about \mathbf{n} gives $\mathbf{n}=\mathbf{k}$, $\mathbf{b}=\mathbf{j}$ and $\mathbf{t}=-\mathbf{i}$.

With $T(s, t)$ as the tension and $u_t(s, t)$, $u_n(s, t)$ and $u_b(s, t)$ as the velocity

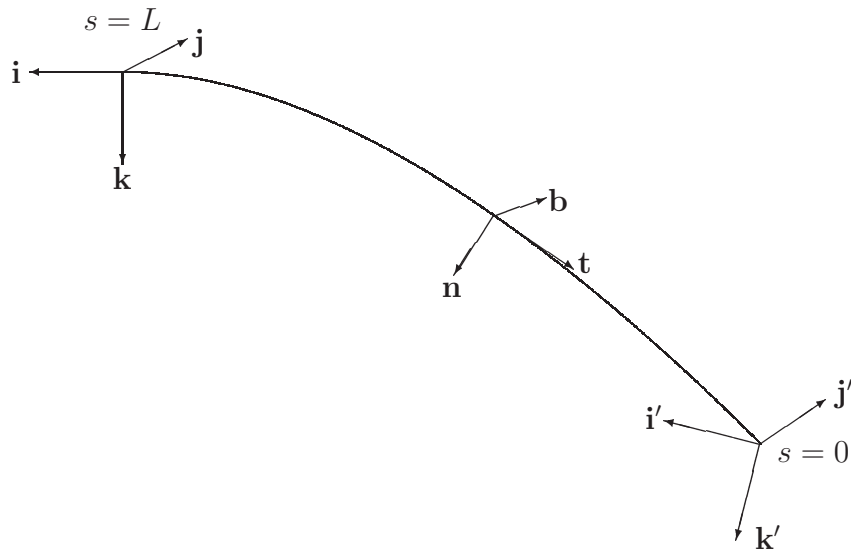


FIGURE 1: The three reference frames used in the model.

components, the governing equations can be written as

$$\frac{\partial T}{\partial s} = \frac{\mu e u_t}{1 + eT} \frac{\partial T}{\partial t} - \mu \frac{\partial u_t}{\partial t} - \mu u_b \cos \phi \frac{\partial \theta}{\partial t} + \mu u_n \frac{\partial \phi}{\partial t} + f_t, \quad (1)$$

$$\begin{aligned} \frac{\partial \theta}{\partial s} = & \frac{-\mu e u_b}{T(1 + eT) \cos \phi} \frac{\partial T}{\partial t} + \frac{\mu}{T \cos \phi} \frac{\partial u_b}{\partial t} \\ & - \frac{\mu(u_t - u_n \tan \phi)}{T} \frac{\partial \theta}{\partial t} + \frac{f_b}{T \cos \phi}, \end{aligned} \quad (2)$$

$$\frac{\partial \phi}{\partial s} = \frac{\mu e u_n}{T(1 + eT)} \frac{\partial T}{\partial t} + \frac{\mu u_b \sin \phi}{T} \frac{\partial \theta}{\partial t} - \frac{\mu}{T} \frac{\partial u_n}{\partial t} - \frac{\mu u_t}{T} \frac{\partial \phi}{\partial t} - \frac{f_n}{T}, \quad (3)$$

$$\begin{aligned} \frac{\partial u_t}{\partial s} = & e \left[\frac{\mu(u_n^2 + u_b^2)}{T(1 + eT)} - 1 \right] \frac{\partial T}{\partial t} - \frac{\mu u_n}{T} \frac{\partial u_n}{\partial t} - \frac{\mu u_b}{T} \frac{\partial u_b}{\partial t} \\ & + \frac{\mu u_b u_t}{T} \cos \phi \frac{\partial \theta}{\partial t} - \frac{\mu u_t u_n}{T} \frac{\partial \phi}{\partial t} - \frac{u_n}{T} f_n - \frac{u_b}{T} f_b, \end{aligned} \quad (4)$$

$$\begin{aligned} \frac{\partial u_n}{\partial s} = & \frac{-\mu e}{T(1 + eT)} \left(u_t u_n + u_b^2 \tan \phi \right) \frac{\partial T}{\partial t} + \frac{\mu u_t}{T} \frac{\partial u_n}{\partial t} \\ & + \frac{\mu u_b \tan \phi}{T} \frac{\partial u_b}{\partial t} - \frac{\mu u_b}{T} \left(2u_t - u_n \tan \phi \right) \sin \phi \frac{\partial \theta}{\partial t} \\ & + (1 + eT) \left[\frac{\mu u_t^2}{T(1 + eT)} - 1 \right] \frac{\partial \phi}{\partial t} + \frac{u_t}{T} f_n + \frac{u_b}{T} \tan \phi f_b, \end{aligned} \quad (5)$$

$$\begin{aligned}
\frac{\partial u_b}{\partial s} = & \frac{-\mu e u_b}{T(1+eT)} \left(u_t - u_n \tan \phi \right) \frac{\partial T}{\partial t} + \frac{\mu}{T} \left(u_t - u_n \tan \phi \right) \frac{\partial u_b}{\partial t} \\
& - (1+eT) \cos \phi \left[\frac{\mu}{T(1+eT)} (u_t - u_n \tan \phi)^2 - 1 \right] \frac{\partial \theta}{\partial t} \\
& + \frac{(u_t - u_n \tan \phi)}{T} f_b,
\end{aligned} \tag{6}$$

where

$$\begin{aligned}
f_t &= \mu g \sin \phi - \frac{1}{2} \rho \pi d_0 \sqrt{1+eT} c_t u_t |u_t|, \\
f_n &= -\mu g \cos \phi + \frac{1}{2} \rho d_0 \sqrt{1+eT} c_n u_n \sqrt{u_n^2 + u_b^2}, \\
f_b &= \frac{1}{2} \rho d_0 \sqrt{1+eT} c_n u_b \sqrt{u_n^2 + u_b^2},
\end{aligned}$$

and μ is the mass per unit length of the unstretched cable, ρ is the air density, d_0 is the diameter of the unstretched cable, c_t and c_n are the tangential and normal drag coefficients of the cable, g is gravitational acceleration, and $e = (EA)^{-1}$ where E is Young's modulus of elasticity and A is the cross-sectional area of the unstretched cable. These six partial differential equations ensure conservation of linear momentum and compatibility of the displacements of the cable; their derivation may be found in [5].

The cable's velocity at the aircraft end ($s = L$, where L is the unstretched length of the cable) is the sum of the velocity of the aircraft and the cable deployment or retrieval velocity $u_c(t)$. If the aircraft's velocity components

in the \mathbf{i} , \mathbf{j} and \mathbf{k} directions are denoted by U , V and W respectively, then

$$\begin{aligned}u_t &= -U \cos \theta \cos \phi - V \sin \theta \cos \phi + W \sin \phi + u_c, \\u_n &= U \cos \theta \sin \phi + V \sin \theta \sin \phi + W \cos \phi, \\u_b &= -U \sin \theta + V \cos \theta.\end{aligned}$$

The variables that define the motion of the towed body are expressed in terms of body axes $x'y'z'$ which move with the towed body. The origin of the body axes is located at the centre of mass of the towed body, the x' axis is aligned with the centreline and points forward, while the y' axis lies in a horizontal plane and the z' axis lies in a vertical plane when the aircraft is flying on a straight and level course at constant speed and cable-body system is in its equilibrium position. The orientation of the towed body is defined by the Euler angles ϑ , φ and ψ , the pitch, roll and yaw angles respectively, which relate the body axes to the fixed axes. To obtain the orientation of the body axes from the fixed axes requires a rotation of ψ about the z' axis, followed by a rotation of ϑ about the y' axis then φ about the x' axis.

The equations of motion of the towed body arise from the conservation of both linear and angular momentum. The components of velocity are denoted by u , v and w and the rates of rotation about the axes are denoted by p , q and r . The following expressions for the time derivatives of state variables

can be derived from the equations of motion (see [6]):

$$\dot{u} = rv - qw - g \sin \vartheta + \frac{X}{m}, \quad (7)$$

$$\dot{v} = -ru + pw + g \cos \vartheta \sin \varphi + \frac{Y}{m}, \quad (8)$$

$$\dot{w} = qu - pv + g \cos \vartheta \cos \varphi + \frac{Z}{m}, \quad (9)$$

$$\dot{p} = \frac{I_{xz}(I_{xx} + I_{zz} - I_{yy})pq + (I_{yy}I_{zz} - I_{zz}^2 - I_{xz}^2)qr + I_{zz}L + I_{xz}N}{I_{xx}I_{zz} - I_{xz}^2}, \quad (10)$$

$$\dot{q} = \frac{(I_{zz} - I_{xx})pr - I_{xz}(p^2 - r^2) + M}{I_{yy}}, \quad (11)$$

$$\dot{r} = \frac{(I_{xx}^2 + I_{xz}^2 - I_{xx}I_{yy})pq + I_{xz}(I_{yy} - I_{xx} - I_{zz})qr + I_{xz}L + I_{xx}N}{I_{xx}I_{zz} - I_{xz}^2}, \quad (12)$$

$$\dot{\psi} = \frac{q \sin \varphi + r \cos \varphi}{\cos \vartheta}, \quad (13)$$

$$\dot{\vartheta} = q \cos \varphi - r \sin \varphi, \quad (14)$$

$$\dot{\varphi} = p + \dot{\psi} \sin \vartheta. \quad (15)$$

Here m is the mass of the towed body, X, Y and Z are the components of aerodynamic force, L, M and N are moments about the body axes and I_{xx}, I_{yy}, \dots are second moments of inertia about the indicated axes. The components of force and the moments are calculated by adding perturbations

to the steady state values and any contributions from the cable. For example,

$$X = f_{A_x} - \frac{1}{2}\rho U_1^2 S C_{D_1} + T \cos(\theta(0, t) - \vartheta)$$

where f_{A_x} is the perturbed force in the x direction and U_1 and C_{D_1} are the speed and the drag coefficient at steady state flight conditions. Perturbations to the forces and moments are found using a linear approximation (see [6]).

3 Numerical Scheme

The six coupled partial differential equations that govern the motion of the cable are discretised using the finite difference method. The cable is divided into a number of elements whose length increases geometrically from the towed body end (where the curvature is greatest) to the aircraft end. An implicit approximation that is second order in both space and time was first developed in [4] for motion of an inelastic cable constrained to move in a vertical plane. Details of the scheme applied to equations (1) to (6) may be found in [5].

Equations (7) to (15) are discretised using the backward Euler method. Using the notation that variables without a superscript are approximations at some time $t_r = r\Delta t$ and those with a superscript of '+' are approximations at time $t_{r+1} = t_r + \Delta t$, Equation (7) is approximated by

$$\frac{u^+ - u}{\Delta t} = r^+ v^+ - q^+ w^+ - g \sin \vartheta^+ + \frac{X^+}{m}.$$

The cable end and the towed body must move at the same velocity. Equating expressions for the velocity components of each in the fixed coordinate system gives

$$\begin{aligned} & \left[\begin{array}{l} u \cos \vartheta \cos \psi + \cos \varphi (w \cos \psi \sin \vartheta - v \sin \psi) + \sin \varphi (v \cos \psi \sin \vartheta + w \sin \psi) \\ (u \cos \vartheta + v \sin \vartheta \sin \varphi) \sin \psi + \cos \varphi (v \cos \psi + w \sin \vartheta \sin \psi) - w \cos \psi \sin \varphi \\ -u \sin \vartheta + \cos \vartheta (w \cos \varphi + v \sin \varphi) \end{array} \right] \\ & = \left[\begin{array}{l} -u_{t_1} \cos \theta_1 \cos \phi_1 + u_{n_1} \cos \theta_1 \sin \phi_1 - u_{b_1} \sin \theta_1 \\ -u_{t_1} \sin \theta_1 \cos \phi_1 + u_{n_1} \sin \theta_1 \sin \phi_1 + u_{b_1} \cos \theta_1 \\ u_{t_1} \sin \phi_1 + u_{n_1} \cos \phi_1 \end{array} \right], \end{aligned}$$

where the subscript 1 denotes values at the first node ($s = 0$). This equation is enforced at each time level.

The discretisation of the governing equations together with the equations for the velocity at the cable ends form a system of non-linear equations that must be solved at each time step. This system is solved iteratively using Broyden's method [3].

The simulation of the cable-body system is started with the aircraft flying in a straight line at a constant altitude and the cable and towed body in their equilibrium positions. First the equilibrium position of the towed body is found. Expressions relating T , θ_1 and ψ at equilibrium are solved by a fixed point iterative scheme with under-relaxation. Numerical experiments showed that rapid convergence was achieved for a relaxation parameter of 0.38. Once

the equilibrium orientation of the towed body has been found, the steady form of equations (1) to (6) are integrated to determine the equilibrium position of the cable.

4 Results

The following results were calculated for a cable of diameter $d = 2\text{mm}$ with tangential drag coefficient $c_t = 0.01$ and normal drag coefficient $c_n = 0.5$. A mass per unit length of cable of $\mu = 30\text{g/m}$ and the value $e = 1.516 \times 10^{-6}$ (corresponding to a steel cable) was used. The mass of the module was $m = 31\text{kg}$. The air density was assumed to be $\rho = 1.22\text{kg/m}^3$. Experimentation showed that a ratio of 1.15 for the lengths of adjacent elements gave the best accuracy. A time step of $\Delta t = 0.1\text{s}$ was used as any further reduction made little difference to the results.

The first simulation is for the aircraft in a circular flight. The cable is initially 500 metres long. Figure 2 shows the path taken by the aircraft and the module in the xy plane. The dotted line represents the path taken by the module and the other the aircraft's flight. Initially the aircraft is at $(0, 0)$ moving with velocity 150m/s in the direction of the x -axis and towing the module from a cable of length 500 metres. At time $t = 10$ seconds, the cable payout is initiated with a payout speed which increases linearly to 10m/s after 10 seconds. At the same time, the aircraft, now positioned at $(1500, 0)$, commences a turn. As shown in the figure, the module travels outside the

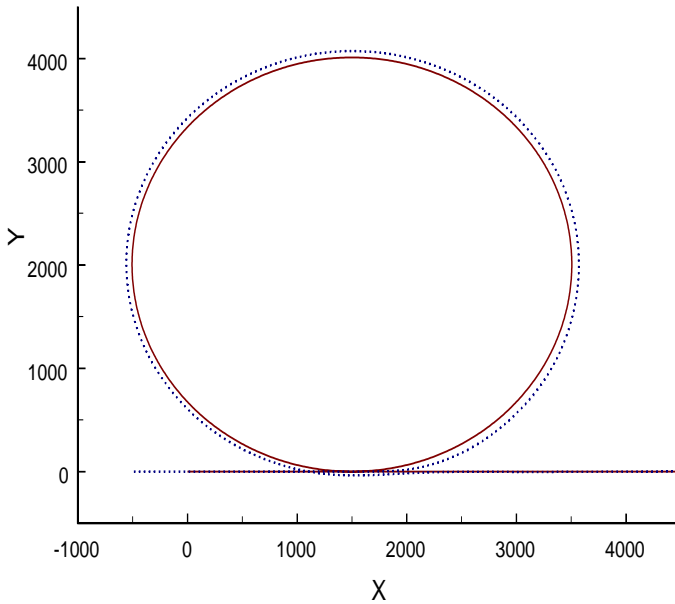


FIGURE 2: Aircraft path (solid line) and module path (dotted line) during deployment of cable.

path taken by the aircraft. The payout velocity is maintained at 10m/s for t between 20 and 110 seconds. When the circle is completed at time $t = 94$ seconds, the aircraft continues to fly in a straight line. At time $t = 110$ seconds, the payout velocity of the cable is decreased linearly to zero at time $t = 120$ seconds. The final length of the cable is 1500 metres. The number of nodes on the cable was initially 31. At the end of the payout, the number of nodes increased to 39.

Figure 3 shows the tension at each end of the cable. Initially, the tension is slightly higher at the aircraft end than at the module end. As the cable is payed out, the tensions initially decrease, then fluctuate, and as the cable becomes longer, the tension at the aircraft end increases. The tension at the module end settles down to a constant value. Fluctuations in the tensions are observed when the aircraft begins to fly in a straight path. As the cable is slowed, the rate of change in tension at the aircraft end increases until the payout ceases. Once the payout of the cable is stopped, the tensions quickly reach their equilibrium values. The oscillations at $t = 10$ s and $t = 94$ s result from the discontinuity in acceleration when the “aircraft” changes from a straight path to a circular path and vice versa.

The next manoeuvre (see Figure 4) is the same except at $t = 10$ seconds, as the plane begins to turn, it starts to ascend. After 1 second, the rate of ascent reaches 5m/s and this value is maintained for the rest of the simulation. The tensions graph are shown in Figure 5. The effect of the aircraft climbing is minimal, the tensions being very similar to those from the earlier manoeuvre.

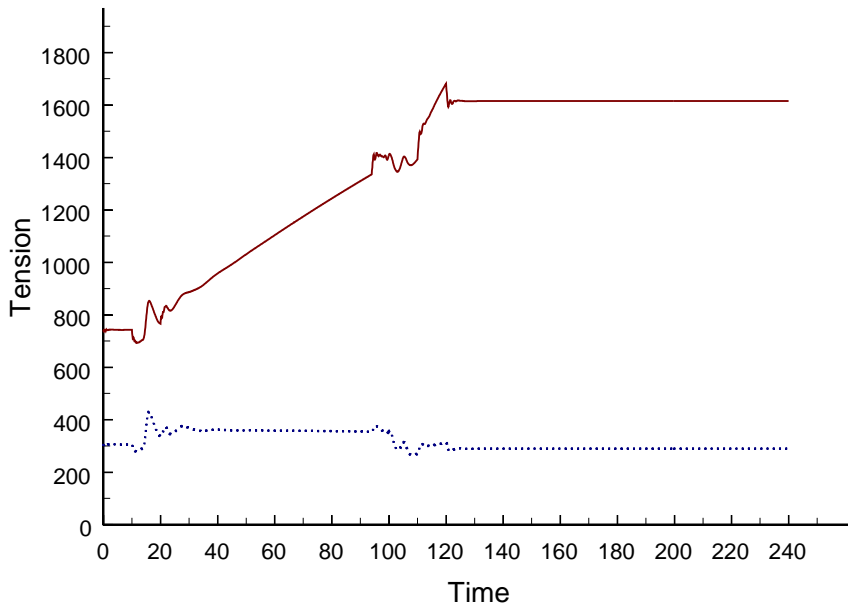


FIGURE 3: Tension in cable at aircraft end (solid line) and module end (dotted line) during manoeuvre shown in Figure 2.

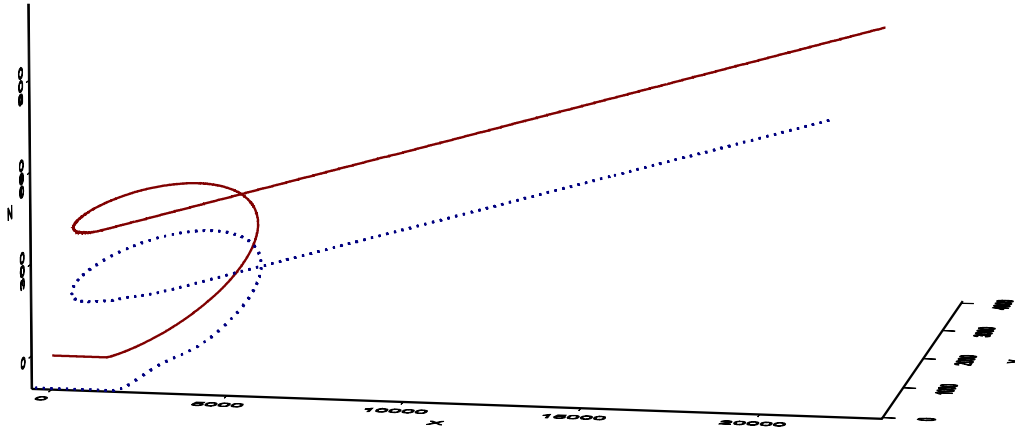


FIGURE 4: The aircraft path (solid line) and module path (dotted line) during deployment of the cable.

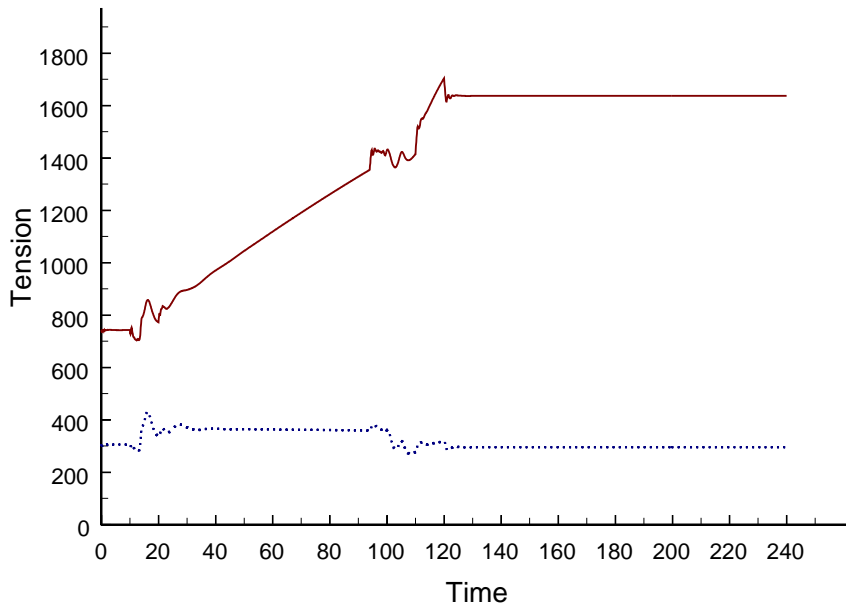


FIGURE 5: The tension in the cable at the aircraft end (solid line) and module end (dotted line) during the manoeuvre shown in Figure 4.

Figure 6 shows a manoeuvre which involves retrieval of a 500m long cable. Initially, the aircraft is flying at a constant speed of 150m/s. At time $t = 10$ seconds, the aircraft commences to turn and climb. The rate of climb increases from 0 to 5m/s over a period of one second, then is maintained at 5m/s for the rest of the manoeuvre. The aircraft completes a semicircle at time $t = 52$ seconds and returns to straight flight, on an opposite heading than at the start of the manoeuvre. The retrieval of the cable commenced at time $t = 10$ seconds. The retrieval velocity is

$$u_c(t) = \begin{cases} -7.5 \{1 - \cos [\pi(t - 10)/10]\} & 10 \leq t < 20 \\ -15 & 20 \leq t < 30 \\ -7.5 \{1 - \cos [\pi(t - 40)/10]\} & 30 \leq t < 40 \\ 0 & \text{otherwise.} \end{cases}$$

This results in 300m of cable being reeled in.

Figure 7 shows the tension for this manoeuvre. Initially, the tension oscillates insignificantly before reaching a steady value. When the aircraft commences its turn and the retrieval begins, the tension at both the aircraft and module increases dramatically. At $t = 20$ seconds, the rate of retrieval becomes steady and we observe tension at the aircraft end drops quickly while at the module end the rate of decrease is much smaller. As the retrieval velocity is reduced to zero the tensions level off. The tensions at both ends of the cable have some large fluctuations which begin at time $t = 52$ seconds, when the aircraft ceases its turn, before settling down to a lower value. The module oscillates from side to side of the aircraft's path after the aircraft straightens up (see Figure 8), but the period of the oscillation is much greater

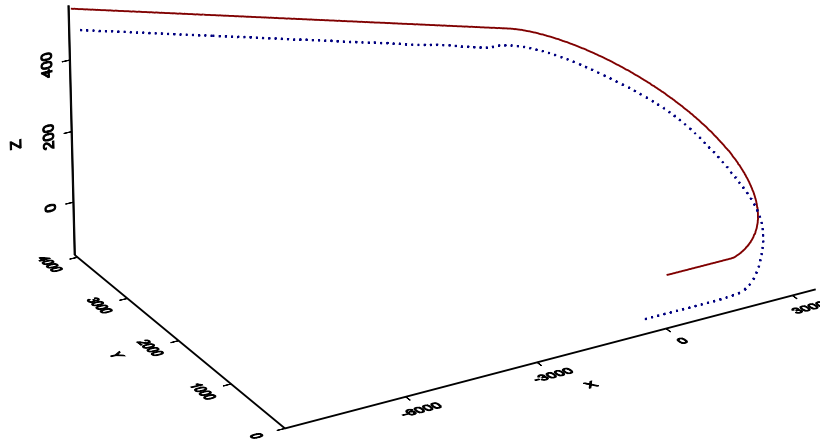


FIGURE 6: The aircraft path (solid line) and module path (dotted line) during retrieval of the cable.

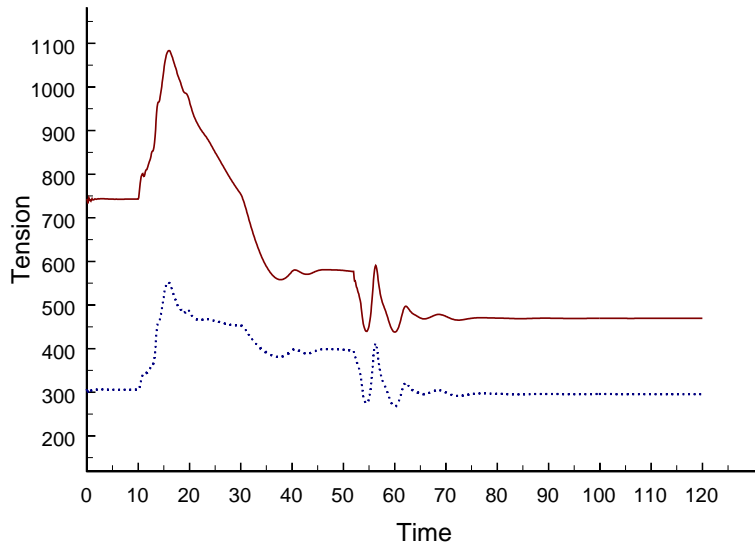


FIGURE 7: The tension in the cable at the aircraft end (solid line) and module end (dotted line) during the manoeuvre shown in Figure 6.

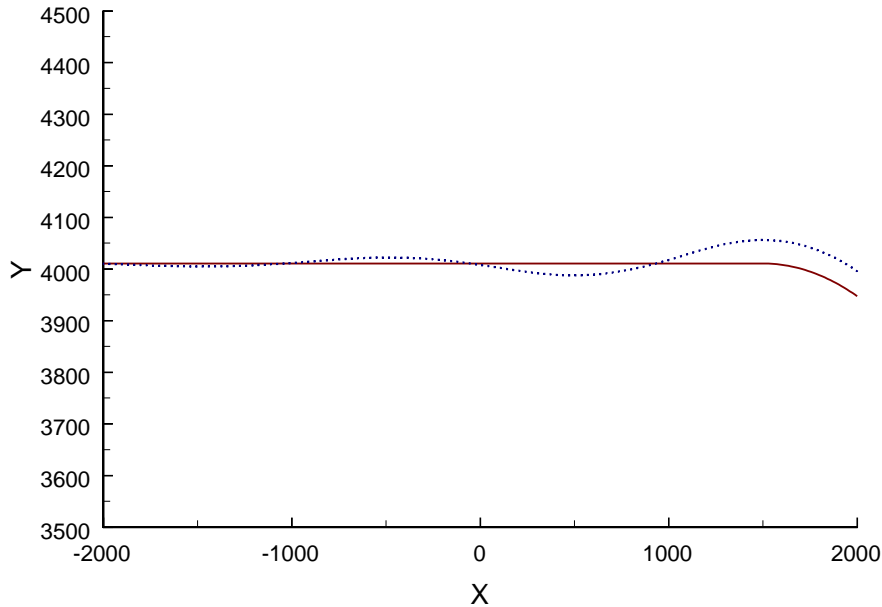


FIGURE 8: Expanded view of a section of the aircraft path (solid line) and module path (dotted line) displayed in Figure 6.

than the period of the oscillation of the tensions; the latter oscillation is again caused by the discontinuity in the acceleration of the aircraft end of the cable.

5 Conclusions

The incorporation of a six degree of freedom model of the module has improved the accuracy of the model of a towed cable–body system. At present the path of the aircraft has to be defined by specifying the aircraft’s velocity components as functions of time, and any discontinuity in acceleration results in oscillations of the tension in the cable. In the future it is planned to incorporate a model of the aircraft. This will not only eliminate the spurious oscillations, but will also allow interaction between the aircraft and the towed system.

References

- [1] C. M. Ablow and S. Schechter. Numerical simulation of undersea cable dynamics. *Ocean Engineering*, 10:443–457, 1983. C364
- [2] A. K. Banerjee. Dynamics of tethered payloads with deployment rate control. *Journal of Guidance and Control*, 13:759–762, 1990. C364

- [3] C. G. Broyden. A class of methods for solving nonlinear simultaneous equations. *Mathematics of Computation*, 19:577–593, 1965. C372
- [4] R. L. May and H. J. Connell. Towed systems modelling study. RMIT Department of Mathematics Technical Report No. 10, Melbourne, 1988. C364, C371
- [5] G. M. Roberts, H. J. Connell, and R. L. May. A three dimensional model of a towed cable-body system. RMIT Department of Mathematics Research Report No. 14, Melbourne, 1994. C368, C371
- [6] J. Roskam. Airplane flight dynamics and automatic flight controls. Design, Analysis and Research Corporation, 1995. C370, C371
- [7] P. J. Wingham and B. Ireland. The dynamic behaviour of towed airborne and underwater body-cable systems. *Advances in Water Technology, Ocean Science and Offshore Engineering*, 15:17–30, 1988. C364